

The Torque and X-Ray Flux Changes of
OAO 1657-415

Altan Baykal

Laboratory for High Energy Astrophysics NASA /G SFC Greenbelt, Maryland 20771 USA

NAS/NRC Resident Research Associate,

Physics Department, Middle East Technical University, Ankara 06531, Turkey

Received _____; accepted _____

A B S T R A C T

Combining previously published pulse frequencies and BATSE measurements, we estimate the noise strengths (or power density estimates) of angular accelerations by using the root mean square residuals of angular velocity time series of OAO 1657-415 and present the power spectra. The statistical interpretation of the angular velocity fluctuations are consistent with a random walk model. In order to investigate the short term angular velocity fluctuations in detail, a structure function analysis is applied for a two component neutron star model with a solid crust and a superfluid neutron core which is subjected to external white torque noise. No evidence for core-crust coupling on timescales longer than one day is found. The correlations between X-ray flux and angular acceleration ($\dot{\omega}$) fluctuations are investigated. These are compared with disk accretion theory (Ghosh & Lamb 1979 a,b) and wind accretion theory (Blondin et al., 1990). It is found that the most natural explanation of X-ray flux and angular acceleration fluctuations is the formation of episodic accretion disks in the case of stellar wind accretion.

1. Introduction

The X-ray source OAO 1657-415 was first detected by the Copernicus satellite (Polidan et al. 1978) in the 4-9 keV range. Initially association of this source with a massive star V861 Scorpii was considered. Subsequent observations by HEAO 1 satellite (Byrne et al. 1979; Armstrong et al. 1980) and the Einstein Observatory (Parmar et al. 1980) did not confirm the association with V861 Scorpii. The HEAO 1 observations also showed 38.22 sec pulsations in the 1-40 keV and 40-80 keV bands (White & Pravdo 1979; Byrne et al. 1981). Observations with Ginga and GRANAT (Kamata et al. 1990; Gilfanov et al. 1991; Mereghetti et al. 1991; Sunyaev et al. 1991) have shown episodic changes in the pulse period. Timing observations of this source with the Burst and Transient Source Experiment (BATSE) on the Compton Gamma Ray Observatory (CGRO) have shown that OAO 1657-415 is in an 11 days binary orbit with an X-ray eclipse by the stellar companion (Chakrabarty et al. 1993). The observed orbital parameters imply that the companion is a supergiant of spectral class B0-B6.

Massive X-ray binaries fall into three separate groups when the pulse periods are compared with orbital periods (Corbet 1986). The systems with Be companions show correlations between the orbital and spin periods (Corbet 1986; Waters & van Kerkwijk 1989), while systems with OB supergiant companions fall into two separate regions. X-ray pulsars with Be companions show transient behavior with episodic spin-ups (i.e. EXO 2030+375, Parmar et al., 1989; A0535+26, Finger et al., 1996) which suggest that the low velocity equatorial stellar wind forms an accretion disk during the periastron passages. Systems with OB giants with pulse periods $P < 10$ sec and orbital periods $P_{\text{orbit}} < 4$ days show optical photometric evidence for accretion disks (LMC X-1, Cen X-3, and SMC X-1) and nearly steady spin-up on longer time scales $> 10^2$ days (Finger et al., 1993). BATSE observations of Cen X-3 have shown a lot of spin-up/down episodes on time scales

$< 10^2$ days, this behaviour in LMC X-1 and SMC X-1 is not known because of the long gaps between adjacent observations. Systems with longer spin periods (> 100 sec) showed short term spin-up/down episodes at < 10 days (i.e Vela X-1, see Deeter et al., 1989) which can be explained in terms of dipole instabilities of wind accretion (or very short time scale accretion disk formation; see Anzer et al., 1987; Matsuda et al., 1987; Blondin et al., 1990). OAO 1657-415 falls between these groups in terms of orbital and spin period. In order to improve our understanding of the spin history and the accretion process of the source, in this work we study the statistical properties of the angular velocity changes and investigate the possible correlations of angular acceleration with X-ray flux.

The angular velocity fluctuations in accretion powered neutron stars are produced by torques originating outside and inside the object. The external torque is carried by the accretion flow; the internal torque depends on the coupling between the core superfluid and the solid outer crust. External fluctuations of the torque are filtered by the coupling between the crust and superfluid interior to produce an output represented by the observed changes in the angular velocity. The theoretical description of torque variations in terms of noise power spectral analysis was first studied by Lamb et al., (1978a,b), who analyzed the response of a two component star to external fluctuations. Their model makes it possible to diagnose theoretically the properties of accretion flows and the internal structure of neutron stars. Techniques for estimating the noise power spectra in the case of nonuniformly sampled pulsar timing data were developed by Deeter & Boynton (1982) and Deeter (1984). They were applied to Vela X-1 and Her X-1 using the data obtained by HEAO-1 and UHURU (Boynton 1981; Deeter 1981; Boynton et al., 1984; Deeter et al., 1989). The results showed that the angular velocity time series of Vela X-1 and Her X-1 can be modelled as a random walk (or white noise in the angular accelerations with a power law index $n = 0$). Recent results of BATSE observations are indicating that 4U 1626-67 has an angular velocity time series which is also consistent with the random walk model (Chakrabarty et

al., 1995). Random walk in angular velocity can be characterized by a rate of torque events R of steps $\Delta\Omega$. The rate and the step size of the events depend on the type of accretion (Prince et al., 1994). For example in the wind accretor Vela X-1, the spin-up/down time scales are around day (Deeter et al., 1989), therefore the rate of the torque events may be $R < 1 \text{ days}^{-1}$ while in Her X-1 the rate is lower due to the disk accretion (Wilson et al., 1994). Time domain techniques such as autoregressive time series (Scargle 1981) were applied by Baykal & Ogelman (1993) and de Kool & Anzer (1993) in order to model the angular velocity time series of accretion powered X-ray binaries. They found that some of these systems have angular velocity time series which are consistent with random walk. Recent BATSE results for Cen X-3 and GX 1+4 have shown that the noise power spectrum is redder than the random walk model in angular velocity time series (or flicker noise in the angular accelerations with power law index $n = 1$; see Finger et al., 1994; Chakrabarty et al., 1995). The reason for flicker noise in the angular accelerations may be the smooth transitions from spin-up to spin-down (or vice versa) (see Finger et al., 1994) which makes the noise power spectra steeper (or redder).

The sign and magnitude of the torque physically depends on the magnetosphere of the neutron star and the type of accretion flow exterior to magnetosphere (Ghosh & Lamb 1979 a,b; Blondin et al., 1990). One way to study the accretion dynamics of neutron stars is to observe the nature of the correlation between changes in rotation rate ($\dot{\Omega}$) and mass accretion rate (\dot{M}) (or the related quantity X-ray flux). Such a study may provide more detailed information on the physics of accretion and helps to discriminate between disk and wind-type accretion (Ghosh & Lamb 1979 a,b; Blondin et al., 1990).

In this paper, we apply various techniques in order to study the torque fluctuations of OAO 1657-415. In Section 2, the data base used in this analysis is described. In Section 3, we construct the low resolution power density spectrum using the mean-squared

residuals technique developed by Cordes (1980) and Deeter (1984). In Section 4, to see the sharp changes of rotation rate, a structure function is calculated Cordes (1980); the two component neutron star model and the response of the neutron star to external white torque noise is compared with the observed data. In Section 5, the correlations between the angular acceleration ($\dot{\omega}$), X-ray flux, and specific angular momentum are studied. These correlations are compared with the disk accretion hypothesis (Ghosh & Lamb 1979 a,b) and the wind accretion hypothesis (Blondin et al., 1990).

2. The Data Base

In this work, we used pulse frequency records compiled from the published literature (Nagase 1989; Gilfanov et al. 1991) and generated from BATSE observations. The total time span of the observations covers approximately 16 yr. The measured angular velocities are plotted as a function of time in Fig. 1. The BATSE detections of angular velocities are plotted in Fig. 2. These records are measured on the basis of daily analysis after removing binary motion of the neutron star and are available through anonymous ftp from HEASARC. The BATSE data base contains 1219 pulse frequency and pulse flux measurements of OAO 1657-415 in a time span of over 3 years. (BATSE instrument has 8 uncollimated detector modules arranged on the corners of the CGRO spacecraft which are sensitive $> 20\text{keV}$; for details of the observatory and observation see Fishman et al., 1989; Chakrabarty et al., 1993). The gaps in Fig. 2 corresponds to either no detection of the source or insignificant detections.

3. Power Spectra

The root mean square residuals technique used in this section for the estimation of red noise power density and associated random walk noise strengths is discussed in detail by Cordes (1980) and Deeter (1984). The applications made by Baykal et al., (1993a,b) are the examples of its use in characterizing random walk processes.

For the case of $r = 1; 2$:th-order red noise (or r th-time integral of white noise time series) with strength S_r , the mean squared residual for data spanning an interval T is proportional to $S_r T^{2r-1}$. The proportionality factor (or normalization coefficient) depends on the degree m of the polynomial removed prior to computing the mean square residual; this factor can be obtained by determining the expected mean square residual for unit strength red noise ($S_r = 1$) over a unit interval ($T = 1$), either by Monte-Carlo methods (Cordes 1980) or by mathematical evaluation (Deeter 1984). The mean square residual, after removing a polynomial of degree m over an interval of length T , is then given by

$$\langle \sigma^2(m; T) \rangle = S_r T^{2r-1} \langle \sigma^2(m; 1) \rangle \quad (1)$$

where $\langle \sigma^2(m; 1) \rangle$ is the proportionality factor which has been derived from a unit-strength noise process. Our preliminary analysis showed that the angular velocity residuals can be characterized by first order red noise (or random walk). This noise process is adopted in computing the normalization coefficients. The normalization coefficient is computed by Monte Carlo simulation, sampling the simulated data as the real data set was sampled (Cordes 1980). Because most of the BATSE data are approximately equally spaced at 1 day intervals, the normalization coefficient differs by no more than 15% from the theoretical prediction for equally spaced data (assuming a sampling interval of one day) as given in Table 1 and 2 of Deeter 1984.

As a next step, time scales are sampled at nearly octave spacings for the power density estimators (Deeter 1984). To do this the entire length of the data is taken as the longest time-scale. Then the intervals are halved successively to get down to the shortest practical

time scale. Intervals with insufficient data points are discarded. The mean squared residuals for the remaining intervals are calculated and converted into the noise strengths ($S_{r=1}$) using Eq. 1. The contributions of the measurement errors have been computed by converting the estimated variances of angular velocities into noise strengths and by employing the identical procedure above.

Estimated noise strengths on each time scale are combined into a single power density estimate ($P_{\omega} = (2\pi f)^2 P_{\omega} = S_{r=1}$, where f is the frequency, Rice (1954); Boynton (1981)) by averaging, and are represented by a frequency equal to the inverse of the time scale. In order to estimate the power density error bars, the effective number of degrees of freedom, for each estimate is determined by generating its statistical distribution by using Monte Carlo simulations of a first order red noise process, sampled in the same way as our angular velocity data (Blackman & Tukey 1958; Deeter & Boynton 1982). Then the power density error bars are computed for a given effective number of degrees of freedom by computing the power density values corresponding to the 16% and 84% points of the χ^2 distribution; these are equivalent to 1 confidence level for a Gaussian (Blackman & Tukey 1958). In Fig. 3, we display the resulting power density estimates (or noise strengths) of the angular acceleration fluctuations.

In the analysis, we have found the crossover frequency between the errors and noise strengths around $f_c \approx 1/(8 \text{ days})$. We have fitted a straight line to the 8 lower octave power density estimates and found $n = 0.02 \pm 0.3$ which is consistent with white noise $n = 0$ in the angular accelerations (\rightarrow) with the mean power density (or noise strength) $S = R \langle \ddot{\theta}^2 \rangle = 8.1 \pm 1.2 \cdot 10^{-16} \text{ rad}^2/\text{sec}^3$.

In order to crudely estimate the step size of the fluctuations $\langle \ddot{\theta}^2 \rangle^{1/2}$ and the rate R of torque events we make use of the autocorrelation of angular acceleration (\rightarrow) time series. We took the numerical time derivative of the angular velocity (\rightarrow) time series at time scales

corresponding to the cross over frequency (see Fig. 7b) and represented the autocorrelation function in Fig. 4. Autocorrelation function of white noise time series can be expressed as (Jenkins & Watts 1968),

$$\langle \tau(t) - \tau(t^0) \rangle = \sigma_w^2 (t - t^0) \quad (2)$$

where σ_w^2 is the white noise variance at zero time lag $t = t^0$. As seen from Fig. 4, actually the autocorrelation function shows correlation for time lags (t) up to 8-19 days.

The step size of the fluctuation during this time scale can be estimated $\langle \tau^2 \rangle = \langle \tau^2 \rangle t^2$. By using the values $\langle \tau^2 \rangle = 7.7 \cdot 10^{22} \text{ rad}^2/\text{sec}^4$ and t , from the autocorrelation function and the random walk noise strength estimate from the power spectrum we estimated the rate of torque events as

$$R = \frac{S}{\langle \tau^2 \rangle} \quad 1=30 \quad 1=5 \text{ days}^{-1} \quad (3)$$

This implies a torque event occurs within $1=R^{-1} = 5-30$ days and lasts $t = 8-19$ days. These events appear as a delta function (or unresolved events) if we are studying the long time scale fluctuations and make the power spectra of τ at low frequency (or long time scales $t \gg t$ days). But at high frequencies (or short time scales $t \sim t$ days), it is quite natural to see decrease in power density estimates. If we express the white noise time series as a sum of Gaussians $\tau = \sum_i \frac{1}{(\sigma_i)^{1/2}} e^{-(t-t_i)^2/(2\sigma_i^2)}$, with a small white noise variance $\sigma_i^2 = t^2$, then we would expect the power spectrum to have the form $P_\tau = R \langle \tau^2 \rangle e^{-2f^2 t^2}$. Therefore at frequencies $f = 1/(2t)^{1/2}$ one should see a decrease in the power spectra at order of e^{-1} . This is qualitatively seen in our low resolution power spectra (see Fig. 3).

4. Structure Function Analysis

In this section we study the short term fluctuations of angular velocities by employing structure function analysis (Lindsey & Chie 1976; Cordes & Downs 1985). This technique is more sensitive to sharp fluctuations. Therefore it is more likely to show the effects of a possible decoupling between the crust and the superfluid core. A first order structure function for the angular velocity time series can be defined as

$$D(\tau_0; \tau) = \langle (\omega(\tau_0 + \tau) - \omega(\tau_0))^2 \rangle : \quad (4)$$

For a random walk in frequency one can express the time series as

$$\omega(t) = \sum_i \Delta\omega_i \theta(t - t_i) \quad (5)$$

where $\Delta\omega_i$ is the step size of events θ is the step function and t_i is the events occur at random times with a rate R . The structure function of the above equation can be written as (Cordes 1985),

$$D(\tau) = \langle \Delta\omega^2 \rangle = R \langle \Delta\omega^2 \rangle \tau = S \tau \quad (6)$$

where τ is the lag between two measurements of ω , S is the random walk noise strength.

If the neutron star has significant superfluid in the core (Lamb et al., 1978a,b; Sauls 1988; Lamb 1991; Datta & Alpar 1993) then the moment of inertia of a neutron star resides mainly in its neutron superfluid core. There is a neutron superfluid also in the inner part of the crust lattice. This crust neutron superfluid carries 10^{-2} of the star's moment of inertia, and is coupled to the rest of the crust on very long time scales, typically extending to years (Alpar et al., 1981; Alpar et al., 1993). The crust superfluid moment of inertia is resolved in radio pulsars which are spinning down due to electromagnetic dipole radiation, as a sudden changes in rotation rate (or glitch events) with a magnitude $\Delta\omega = 10^{-9} - 10^{-6}$ and its time derivative $\dot{\omega} = -10^{-3} - 10^{-2}$ (Lyne 1993; Shemar 1993). These kind of glitches can not be detected in the accretion powered X-ray binaries because the external torque noise

in these systems dominates (Baykal & Swank 1996). Also the internal dynamics of radio pulsars spinning down may be quite different (Alpar 1993). In this work we will not be concerned with the crust superfluid. In the core of the neutron star, the rotating neutron superfluid is coupled to the stellar crust by interactions between the charged particles (electrons and protons) and the quantized vortices. In the case of any change in rotation velocity of the crust the whole charged component (protons, electrons) of the stellar interior is coupled to the crust on a short time scale, typically less than 10 sec (Easson 1979). The angular velocity of the neutron superfluid is determined by the density of quantized vortices. The rotation velocity of the core neutron superfluid will not change unless the quantized vortex lines move radially (outward for spin-down and inward for spin-up). Any fluctuation on the crust creates a force on the vortices because of the relative velocity between the vortex line and charged component. Vortex lines relax with charged particles at dynamical (or at the crust-core coupling time) time scales, which is of the order of $\tau = 100 (m = m_p) P^{-1} \approx 10^2 - 10^4 P^{-1}$, where P is the rotation period of the neutron star, m is the change in mass of proton as a result of its coupling with neutrons (Alpar et al., 1984; Alpar & Sauls 1988).

The above scenario can be approximated with a two component neutron star model (Baym et al., 1969). In this model, one component is the crust-charge particle system, which consists of protons, electrons and the crust with an inertia I_c which rotates with angular velocity ω_c . The second component is the core neutron superfluid, with moment of inertia I_s , which rotates with angular velocity ω_s . Any external torque on the crust creates a lag between ω_s and ω_c . The two components are coupled by a crust-core coupling time τ ,

$$I_c \dot{\omega}_c = N(t) \frac{I_c}{\tau} (\omega_c - \omega_s); \quad (7)$$

$$I_{s-s} = \frac{I_c}{I_c + I_s} (\dots) : \tag{8}$$

Here $N(t)$ is the external torque exerted on the star. From the power spectra in the previous section we found that \dots fluctuations are consistent with white torque noise. We assume that external torque fluctuations are also white noise $N(t) = \sum L_i(t - t_i)$, where $L_i = I \dot{\omega}_i$ is the angular momentum added or subtracted from the star at $t = t_i$. Then the fluctuations of the crust can be expressed (Baykal et al., 1991) as

$$\omega_c = \sum_i L_i(t - t_i) \left(1 + \frac{I_s}{I_c} e^{-(I=I_s)(t - t_i)} \right); \tag{9}$$

where $I = I_s + I_c$ is the moment of inertia of the neutron star. If the neutron star response purely rigid $t \gg \dots$ or $I_s \rightarrow 0$ then the time series behave as a pure random walk in angular velocity (see Eq. 5).

By using the definition of the structure function for the time series above and defining the $\dots = \omega_c(t)$, then the mean square fluctuation of the white noise variable can be written as

$$\langle \omega_c^2 \rangle = \frac{R \langle \dots^2 \rangle}{t} \left(1 + \frac{I_s}{I_c} (1 - e^{-(t - t_0)}) \right)^2 \tag{10}$$

where $t_0 = I_s/I$. At long time lag $t \gg t_0$, angular accelerations fluctuations behaves as $\langle \omega_c^2 \rangle^{1/2} = (R \langle \dots^2 \rangle = t)^{1/2}$, while at short time lag $t \ll t_0$ behaves as $\langle \omega_c^2 \rangle^{1/2} = I/I_c (R \langle \dots^2 \rangle = t)^{1/2}$. This means that in the long time lag limit, the core superfluid couples to the neutron star crust and responds to the external torque with total moment of inertia I . On the other hand in the short time lag neutron star responds to external fluctuations with crust moment of inertia I_c (or with charged particle components) (see also Lamb et al., 1978a,b). In Fig. 5a, we plotted the angular acceleration fluctuations in the case of core superfluid mixture $I_s/I_c = 0.3; 10$ for a crust core coupling time $\dots = 1$ day. In the plot we adapted the noise strength value (S) from the power spectrum as $S = R \langle \dots^2 \rangle = 8.13 \times 10^{-16} \text{ rad}^2/\text{sec}^3$. As it is seen from Fig. 5a, if there is a significant

core superfluidity and even if the crust-core coupling time is relatively short ~ 1 day, the crust response increases the angular acceleration fluctuations up to time lags of tens of days. In other words even if we do not see the torque events on shorter time scales we can resolve the crustal moment of inertia by measuring the angular accelerations and testing with a simple two component neutron star model. In Fig. 5b,c, we simulated 1000 independent time series in the form of Eq. 9, is sampled according to the OAO 1657-415 angular velocity history (see Fig. 2). Then we compared the angular acceleration fluctuations with observed fluctuations. In the simulation, we sampled the events uniformly with a rate $R = 1/18 \text{ days}^{-1}$ and used the input variance $\langle \dot{\omega}^2 \rangle = S = R = 1.25 \times 10^{-9} \text{ rad}^2/\text{sec}^2$. First, we simulated the time series with $I_s = I_c = 10$; and $\tau = 1$ day; the simulated angular frequency fluctuations (with larger error bars) are shown together with the observed fluctuations (with smaller error bars) in Fig. 5b. Clearly the simulated fluctuations are not compatible with the observed fluctuations. In Fig. 5c, a pure random walk time series (or a rigid body response with $I_s = I_c = 0$) is simulated. In this case, the simulated and observed angular frequency fluctuations agreed with each other at 1σ level at all time lags (see Fig. 5c). This indicates that the angular acceleration fluctuations seen in OAO 1657-415, are associated with external torques. The absence of a signature of core superfluidity is suggesting us that either crust-core coupling time is so short (i.e. $\tau \ll 1 \text{ days} \sim 2273P$ where $P = 38 \text{ sec}$ is the pulse period) that all charged components and the core superfluid couple on the order of hours or the core superfluidity is not significant $I_s \ll I_c$. If the latter possibility is correct, this is suggesting that either most of the neutrons in the core are too hot to be in the superfluid phase (Answorth et al., 1989) or the equation of state is stiff with higher crustal moment of inertia (Lamb 1991). The well studied high mass X-ray binary Vela X-1 showed that less than 85% of the moment of inertia of the star is weakly coupled to crust with coupling times in the range $(305 - 9159)P$, $P = 283 \text{ sec}$ (Boynton et al., 1984; Baykal et al., 1991) while radio observations constrain the crust-core coupling

time to be $< 1350P$ (Chau 1993).

5. The correlations between Angular Acceleration, Flux and Specific Angular Momentum

In this section, we study the various physical correlations between angular acceleration and mass accretion rate (or pulse flux). The BATSE instrument has a response 20–60 keV (Fishman et al., 1989). Therefore the pulse flux time series which is represented in Fig. 7a, may not represent the bolometric X-ray flux (White et al., 1983). The bolometric X-ray flux L_x erg=sec is related to mass accretion rate \dot{M} ,

$$L_x = \eta G M \dot{M} / R \tag{11}$$

where η is the efficiency factor, G is the gravitational constant, M is the mass of neutron star, R is the radius of the neutron star. In order to understand qualitatively whether the X-ray pulse flux fluctuations are related with mass accretion rates, we represent the autocorrelation function of pulse flux time series in Fig. 6. As it is seen from the Fig. 6, the pulse flux fluctuations are becoming uncorrelated at longer time lags than > 20 days. This time scale is close to that which is obtained from the angular acceleration ($\dot{\omega}$) time series. This suggests that mass accretion episodes are lasting tens of days and giving a certain angular momentum to the neutron star. Therefore the angular accelerations are changing on similar time scales. The way of transferring angular momentum gives us information about the accretion process.

The torque on the neutron star ($\tau < \tau_m$, where τ and τ_m is the crust core coupling time and torque measuring time respectively) can be expressed as a specific angular momentum (l) added to neutron star at some radius with a certain mass accretion rate

(Lamb 1991),

$$\dot{I} = \dot{M} l; \quad (12)$$

If the accretion is from a Keplerian disk (Ghosh & Lamb 1979a,b) then the external torque is given by

$$\dot{I} = n (w_s) \dot{M} l_k; \quad (13)$$

where $l_k = (GM/r_o)^{1/2}$ is the specific angular momentum added by a Keplerian disk to the neutron star at the inner disk edge $r_o = 0.5r_A$; $r_A = (2GM)^{1/2} (4\pi)^{-1/2} \dot{M}^{-1/2}$ is the Alfvén radius; I is the neutron star magnetic moment; $n(w_s) = 1/4 (1 - w_s/w_c) = (1 - w_s)$ is a dimensionless function that measures the variation of the accretion torque as estimated by the fastness parameter $w_s = \dot{\phi}_k(r_o) = 2\pi^{1/2} G^{1/2} M^{-5/2} \dot{M}^{-3/2}$. Here w_c is the critical fastness parameter at which the accretion torque is expected to vanish ($w_c = 0.35 - 0.85$ depending on the electrodynamics of the disk, Lamb 1989). In this model, the torque will cause a spin-up if the neutron star is rotating slowly ($w_s < w_c$) in the same sense as the circulation in the disk, or down, if it is rotating in the opposite sense (see Lamb 1991). Even if the neutron star is rotating in the same sense as the disk flow, the torque will spin-down if it is rotating too rapidly ($w_s >> w_c$). In this model one should see positive correlation between angular acceleration ($\dot{\phi}$) and mass accretion rate (\dot{M}) if the disk is rotating in the same sense as the neutron star. If the flow is from Roche Lobe overflow then the accreting material carries positive specific angular momentum l , therefore it is hard to imagine accretion flow reversals and hence the spin-up/down torques should be correlated with mass accretion rate \dot{M} . Recent numerical simulations indicate that capture from winds may lead to strong circulations at the magnetospheric boundary (or Alfvén surface) which reverses its sign quasiperiodically (Blondin et al., 1990). The formation of Keplerian disks at the magnetospheric boundary is possible (Lamb 1991). Even if the mass accretion is not changing significantly it is possible to see transitions from $+l_k$ to $-l_k$ (or vice versa) and hence to observe spin-up/down episodes.

In general variations in the angular acceleration can be expressed in terms of variations of mass accretion rate \dot{M} and specific angular momentum l

$$\frac{\ddot{\theta}}{\dot{\theta}} = \frac{\dot{M} - l + \dot{M} - l}{I} \quad (14)$$

The mutual correlations of angular acceleration, mass accretion rate and specific angular momentum can give information about whether the accretion is due to Roche Lobe overflow or a stellar wind. In Fig 7a,b,c, we represent the angular acceleration, pulse $\dot{\theta}$ (or mass accretion rate) and the ratio of angular acceleration to pulse $\dot{\theta}$ (or specific angular momentum) time series.

In Fig. 8 a,b,c, we represent the mutual correlations of angular acceleration, pulse $\dot{\theta}$, and specific angular momentum. As seen from Fig. 8a, there is no clear correlation between X ray $\dot{\theta}$ and angular acceleration. In the case of steady accretion disk models (Ghosh & Lamb 1979,b), the higher accretion rate is the higher angular acceleration. But Fig 8a, suggest the opposite case, when the accretion rate is increased angular acceleration is decreased. Furthermore, at all $\dot{\theta}$ values angular acceleration can take both positive and negative sign. In Fig 8b, we represented the specific angular momentum versus pulse $\dot{\theta}$ (or mass accretion). In this case the specific angular momentum goes to zero when the $\dot{\theta}$ increases. For the lower values of $\dot{\theta}$, specific angular momentum has both positive and negative sign. In the case of Keplerian disks the specific angular momentum depends weakly on the X ray $\dot{\theta}$: $l_k \propto L_x^{-1/7}$. When the mass accretion rate is increased, the Alfvén radius gets smaller, therefore a decrease in the specific angular momentum is expected. But it is unlikely to have zero specific angular momentum at higher luminosities. This is suggesting that at higher accretion rates the flow geometry is changing. Possibly the accretion is becoming radial and dumping the material onto the neutron star. On the other hand at lower $\dot{\theta}$ values, the specific angular momentum has both positive and negative sign and the absolute magnitude of specific angular momentum is increased. This suggests

that Keplerian disks form at lower accretion rates and these disks can have both positive and negative circulations. In Fig 8c, we represent the correlation between specific angular momentum and angular accelerations. There is a strong correlation between specific angular momentum and angular acceleration. The above correlations imply that the specific angular momentum is directional, sometimes positive and sometimes negative (or 0), and that sometimes the flow is radial. These results suggest the formation of accretion disks in the case of stellar wind accretion and the short term disk reversals are quite possible.

In the hydrodynamical simulations of nonaxisymmetric gas with transverse velocity and density gradients (or accretion from inhomogeneous stellar wind) flowing onto a gravitating compact object, the formation of a disk and reversals of circulations in the disk are seen (Taam & Fryxell 1988a,b; Taam & Fryxell 1989; Blondin et al., 1990). These simulations also showed that while the disk is present, the specific angular momentum is high and the mass accretion rate is low. When the disk alternates its sense of rotation, the mass accretion increases rapidly, leading to flare like activity. At MJD 48773 and MJD 49004, the source flux increased rapidly (see Fig. 7a) while the source transitioned from spin-up to spin-down (see Fig. 7b). During these flares the specific angular momentum was very low (see Fig. 7c) (It should be noted that these flares are the highest flux points in Fig. 8a,b). This is very similar to what is seen in hydrodynamical simulations (Taam & Fryxell 1988a,b). In the radiatively driven stellar winds, a fraction of the wind is focused by the gravitational force of the neutron star and shocked in an accretion bow shock. The X-rays emitted from the neutron star heats and photoionizes the wind, and create an ionized gas at the Stromgren zone. This effect slows down the velocity of the gravitationally focused material and increases the density of the wind. This will greatly enhance the mass accretion rate onto the neutron star. The slowly moving high density wind can form a Keplerian disk closer to the neutron star magnetosphere (Blondin et al., 1990). According to the distribution velocity and density gradients, the flow can change

its direction quasiperiodically. The time scale of the flow reversals in the hydrodynamical simulations are of the order of the free fall time scale ($t_{ff} = r_a/v_{rel}$) from the capture radius ($r_a = 2GM/v_{rel}^2$, where v_{rel} is the relative velocity of the wind) (see also Taam & Fryxell 1988a,b; Taam & Fryxell 1989; Blondin et al 1990). This time scale for the slow winds can be ~ 5 days (Blondin et al 1990) which is close to the spin-down episodes seen in OAO 1657-415 angular velocity time series history. It should also be noted that spin-up episodes are longer than the spin-down episodes (see Fig. 2). This is implying that the slowed down dense wind has some specific angular momentum in the sense of orbital motion due to the Coriolis force and this is giving extra spin-up torques rather than spin-down.

6. Conclusion

In this work, we model the angular velocity time series of OAO 1657-415 and characterize the type of accretion (wind or disk). The noise power spectrum and the structure function analysis showed that the angular velocity time series history of OAO 1657-415 is consistent with a random walk model, (with steps at order of several days: $t \sim 8 - 19$ days) and that all the observed fluctuations are associated with external torques. The random walk strength $S \sim 8 - 10^{16} \text{ rad}^2/\text{sec}^3$ is consistent with that found by Baykal & Ogelman (1993), $(0.4 - 5.9) \times 10^{15} \text{ rad}^2/\text{sec}^3$, using the data given by Nagase (1989). This noise level is a decade higher than Cen X-3 and GX 1+4 (Finger et al, 1994; Chakrabarty 1995) and $10^2; 10^3; 10^4$ times higher than Her X-1, Vela X-1, 4U 1626-67 (Boynton 1981; Deeter et al, 1989; Chakrabarty 1995). These are the systems in which the noise power density has been studied in detail (for the other sources' estimates see Baykal & Ogelman 1993). The magnitude of the angular accelerations in the spin-up/down episodes are consistent with systems spinning-up/down rapidly such as SMC X-1 (secular spin-up) and GX 1+4 (secular spin-up before 1980, and secular spin-down after 1984). The

high level of angular accelerations in the spin-up/down episodes suggest that the Keplerian disks are present in these episodes. We have found almost no correlation between angular acceleration and mass accretion rate. The strong correlation between angular acceleration and the specific angular momentum implies that the specific angular momentum is changing its sign randomly, as is seen in hydrodynamical calculations of wind accretion (Blondin et al., 1990). Assuming that mass enters the magnetosphere at the corotation radius ($r_{co} = (GM = \dot{M}^2)^{1/3} \approx 2 \times 10^9$ cm), where the angular momentum is added (or subtracted) according to sign of specific angular momentum ($L_k = (GM r_{co})^{1/2}$), and using the mass accretion rate 10^{17} gm sec⁻¹ (Chakrabarty et al., 1993), and the approximate values obtained for the torque event rate ($R \approx 18$ days⁻¹) and duration of events ($t \approx 14$ days), we obtained the approximate value of the random walk strength as,

$$S = R \langle (\dot{L})^2 \rangle = R \langle (\dot{M} t (GM r_{co})^{1/2} = I)^2 \rangle \approx 8.6 \times 10^{16} \text{ rad}^2 \text{ sec}^{-3} \quad (15)$$

This is close to our random walk noise strength value, indicating the possible formation of episodic Keplerian disks. Note however that the mass accretion rate used here is rather uncertain, since it is based on a luminosity which is calculated indirectly using a value for the pulsed fraction from earlier observations, and a very uncertain distance of 10 kpc based mainly on a high interstellar absorption and a low galactic latitude (Kamata et al. 1990). Eq. 15 also shows that the level of noise strength increases with mass accretion rate.

Our findings are strongly suggesting that OAO 1657-415 has an OB type companion. In the case of a Be type of companion, the accretion disk forms from the low velocity equatorial stellar wind. In this case the orbital velocity of the system is higher than the wind velocity. Therefore the flow has enough initial specific angular momentum, and hence the formed disk should be in the same sign with orbital motion. In this case, it is unlikely to expect disk reversals (or flip-flop instabilities) and one should see positive correlations between angular accelerations and mass accretion rates (Ghosh & Lamb 1979a,b).

One of the important observations to test the idea of formation of disk from the stellar wind is to obtain spectral information and examine the column density (or laments) during the orbital phases. The distribution of ionization lines and column density during the orbital phases will give additional information about accretion process (Blondin et al., 1990).

Acknowledgments

It is a pleasure to thank John Deeter, Pranab Ghosh, Jean Swank for stimulating discussions, Mark Finger and CALTECH team, particularly Brian Vaughan, Depto Chakrabarty, Thomas Prince for supplying the pulse frequency and X-ray flux records during the work. I thank the Compton Gamma Ray Observatory team at HEASARC for the archival data and referee Martijn de Kool for helpful comments. I acknowledge the National Research Council for their support.

References

- Alpar, M. A., Anderson, P. W., Pines, D., Shaham, J., 1981, *ApJ* 249, L29
- Alpar, M. A., Langer, S. A., Sauls, J. A., 1984, *ApJ* 282, 533
- Alpar, M. A., Sauls, J. A., 1988, *ApJ* 327, 723
- Alpar, M. A., Chau, H. F., Cheng, K. S., Pines, D., 1993, *ApJ* 409, 345
- Alpar, M. A., 1993 *The Lives of Neutron Stars*, ed, Alpar, M. A., Kiziloglu, J., van Paradijs, J., NATO/ASI, pg 185
- Anzer, U., Bomer, G., Monaghan, J. J., 1987, *A & A* 176, 235
- Armstrong, J. T., Johnston, M. D., Bradt, H. V., Cowley, A. P., Doxsey, R. E., Griths, R. E.,

- Hesser, J E ., Schwartz, D A ., 1980, ApJ 236, L131
- A insworth, T ., P ines, D ., W am bach, J ., 1989, Phys. Lett. B 222, 173
- Baykal, A ., A lpar, A ., K z lglü ., 1991, A & A 252, 664
- Baykal, A ., O gelm an, H ., 1993, A & A 267, 119
- Baykal, A ., Boynton, P E ., D eeter, J E ., & Scott, M ., 1993a, M N R A S 265, 347
- Baykal, A ., Anderson, S F ., M argon, B . 1993b, A J 106, 2359
- Baykal, A ., Swank, J ., 1996, ApJ 460, 470
- Baym , G ., P ethick, C ., P ines, D ., Ruderm an, M ., 1969, N at 224, 872
- Bryne, P ., et al., 1979, IAU C irc., No. 3368
- Bryne, P ., et al., 1981, ApJ 246, 951
- Blackm an, R B ., Tukey, J W .: 1958, The M easurem ent of Power Spectra, (New York D over)
- Blondin, J M ., K alm ann, T R ., Fryxell, B A ., Taam , R E ., 1990, ApJ 356, 591
- Boynton, P E .: 1981, in: Pulsars, IAU Symposium No. 95, eds W . Sieber and R . W ielebinski,
(D ordrecht: Reidel), 279
- Boynton, P E ., D eeter, J E ., Lamb, F K ., Zylstra, G ., Pravdo, S H ., W hite, N E ., W ood,
K S ., Yentis, D J ., 1984, ApJ 283, L53
- Chakrabarty, D ., et al., 1993, ApJ 403, L33
- Chakrabarty, D .: 1995, PhD thesis, California Institute of Technology
- Chau, H F ., M cCulloch, P M ., N andkum ar, R ., P ines, D ., 1993, ApJ, 413 L113
- Corbet, R D H ., 1986, M N R A S 220, 1047

Cordes, J.M., 1980, *ApJ* 237, 216

Cordes, J.M., Downs, G.S., 1985, *ApJS* 59, 343

Datta, B., Apar, M.A., 1993, *A & A* 275, 210

de Kool, M., Anzer, U., 1993, *MNRAS*, 262, 726

Deeter, J.E., 1981, PhD thesis, University of Washington

Deeter, J.E., 1984, *ApJ* 281, 482

Deeter, J.E., Boynton, P.E., 1982, *ApJ* 261, 337

Deeter, J.E., Boynton, P.E., Lamb, F.K., Zylstra, G., 1989, *ApJ* 336, 376

Eason, I., 1979, *ApJ* 228, 257

Finger, M.H., Wilson, R.B., & Fishman, G.J., 1994, In *Second Compton Symposium*, ed. C.E. Fichtel, N. Gehrels, & J.P. Norris (New York: AIP Press), 304

Finger, M., Wilson, R.B., & Hamon, B.A., 1996, *ApJ* in press

Fishman, G.J., et al., 1989, in *Proc. GRO Science Workshop*, ed. W.N. Johnson (Greenbelt: NASA/GSFC) pg 2

Ghosh, P., Lamb, F.K., 1979a, *ApJ* 232, 259

Ghosh, P., Lamb, F.K., 1979b, *ApJ* 234, 296

Gilfanov, M., Sunyaev, R., Churazov, E., Babalyan, G., Pavlinskii, M., Yamburenko, N., Khavenson, N., 1991, *Soviet Astron. Lett.*, 17, 46

Jenkins, G.M., Watts, D.G., 1968, *Spectral Analysis And Its Applications*, Holden Day

Kamata, Y., Koyama, K., Tawara, Y., Makishima, K., Ohashi, T., Kawai, N., Hatsukade, I., 1990, *PA SJ* 42, 785

- Lamb, F K., Pines, D., Shaham, J., 1978a, *ApJ* 224, 969
- Lamb, F K., Pines, D., Shaham, J., 1978b, *ApJ* 225, 582
- Lamb, F K., 1991, *Frontiers of Stellar Evolution*, ed by D. L. Lambert (Astronomical Society of the Pacific), pp 299–388 (1991)
- Lamb, F K., 1989, *Timing Neutron Stars*, ed. H. Ogelman and E. P. J. van den Heuvel (Dordrecht: Kluwer), p. 649.
- Lindsey, W. C., Chie, C. H., 1976, *IEEE* 64, 1652
- Lyne, A. G., 1993, *The Lives of Neutron Stars*, ed, Alpar, M. A., Kızıloglu, J., van Paradijs, J., NATO / ASI, pg 167
- Matsuda, T., Inoue, M., Sawada, K., 1987, *MNRAS* 226, 785
- Mereghetti, S., et al., 1991, *ApJ* 366, L23
- Nagase, F., 1989, *PASJ* 41, 1
- Parmar, A., et al., 1980, *MNRAS* 193, 49P
- Parmar, A., et al. 1989, *ApJ* 338, 359
- Polidan, R. S., Pollard, G. S. G., Sanford, P. W., Locke, M. C., 1978, *Nat* 275, 296
- Prince, T. A., Bildsten, L., Chakrabarty, D., Wilson, R. B., Finger, M. H., 1994, *In Evolution of X-Ray Binaries*, ed. S. S. Holt and C. S. Day (New York: AIP Press), 235
- Rice, S. O., 1954, *Selected Papers on Noise and Stochastic Processes*. Wax N. (ed.), Dover, London, p. 133
- Rutman, J., 1978, *Proc. IEEE* 66, 1048
- Sauls, J. A., 1988 *Timing Neutron Stars*, ed, Ogelman, H., van den Heuvel, E. P. J., NATO / ASI,

Scargle, J.D., 1981, *ApJS* 45, 1

Shemar, S.L., *The Lives of Neutron Stars*, ed. Alpar, M.A., Kiziloglu, J., van Paradijs, J., NATO/ASI, pg 177

Shapiro, S.L., Lightman, A.P., 1976, *ApJ* 204, 555

Sunyaev, R., Gilfanov, M., Goldum, A., Schmitz-Freyesse, M.C., 1991, *IAU Circ.*, No. 5342

Taam, R.E., Fryxell, B.A., 1988a, *ApJ* 327, L73

Taam, R.E., Fryxell, B.A., 1988b, *ApJ* 335, 862

Taam, R.E., Fryxell, B.A., 1989, *ApJ* 339, 297

Waters, L.B.F., van Kerkwijk, M.H., 1989, *A & A* 223, 196

White, N.E., Pravdo, S.H., 1979, *ApJ* 233, L121

White, N.E., Swank, J.H., Holt, S.S., 1983, *ApJ* 270, 711

Wilson, R.B., Finger, M.H., Pendleton, G.N., Briggs, M., Bildsten, L., 1994, *In Evolution of X-Ray Binaries*, ed. S.S.Holt and C.S.Day (New York: AIP Press), 475

Figure Caption

Fig.1 Angular velocity time series history of OAO 1657-415.

Fig.2 Angular velocity records of BATSE observations (same as Fig.1).

Fig.3 Power spectrum of angular accelerations (or noise strengths, see the text). The

asterisks denote the measurement errors.

Fig.4 Autocorrelation function of angular accelerations time series.

Fig.5 a) Theoretical angular accelerations for a crust core coupling time = 1 day and a ratio of core superfluid moment of inertia to crust moment of inertia $I_s/I_c = 0.3; 10$. b) Simulated angular accelerations (with larger error bars) with = 1 day and $I_s/I_c = 10$ and observed angular accelerations. c) Simulated angular accelerations for pure random walk model (larger error bars) and observed angular accelerations (see also text).

Fig.6 Autocorrelation function of pulse ux time series.

Fig.7 BATSE observations of a) pulse ux, b) angular acceleration (horizontal line denotes the secular spin-up rate), c) angular acceleration/ ux (or specific angular momentum) time series (Note that angular accelerations are obtained in a time span, as an inverse of the crossover frequency = 8 days).

Fig.8 Correlations between a) angular acceleration and pulse ux, b) angular acceleration/ ux (or specific angular momentum) and pulse ux, c) angular acceleration/ ux (or specific angular momentum) and angular acceleration (see also text).

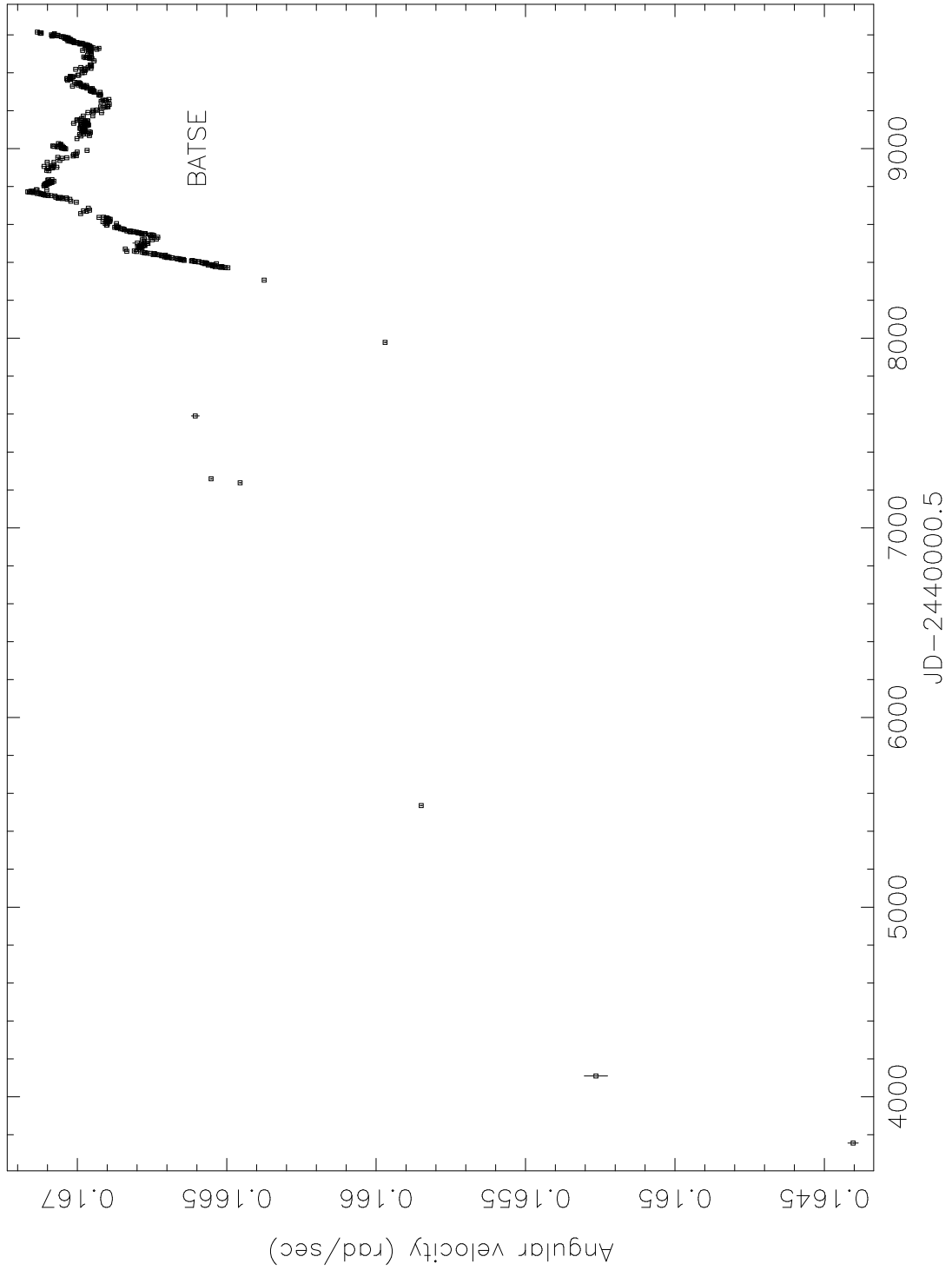


Fig. 1. | Angular velocity time series history of OAO 1657-415

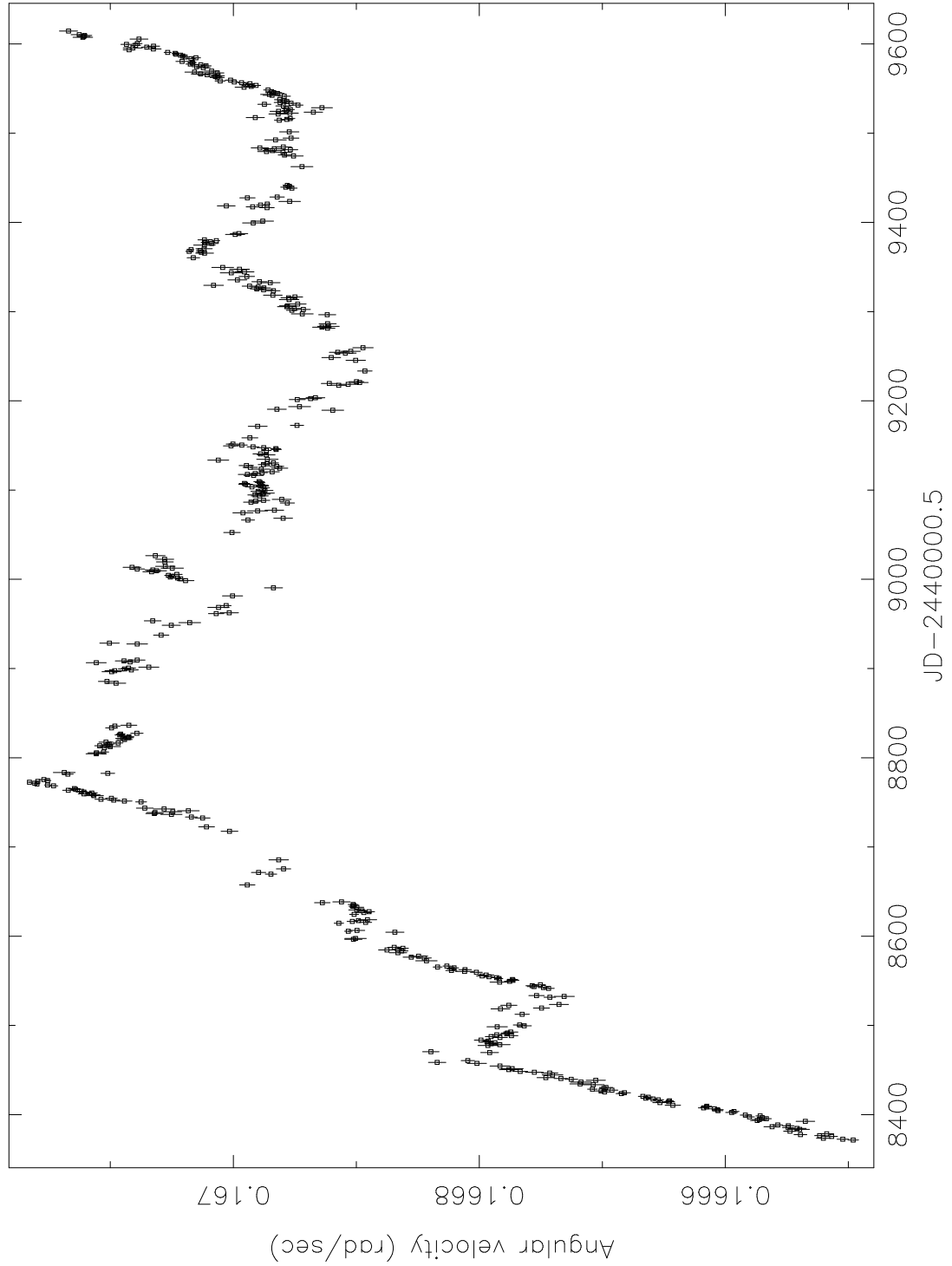


Fig. 2. | Angular velocity records of BATSE observations (same as Fig.1)

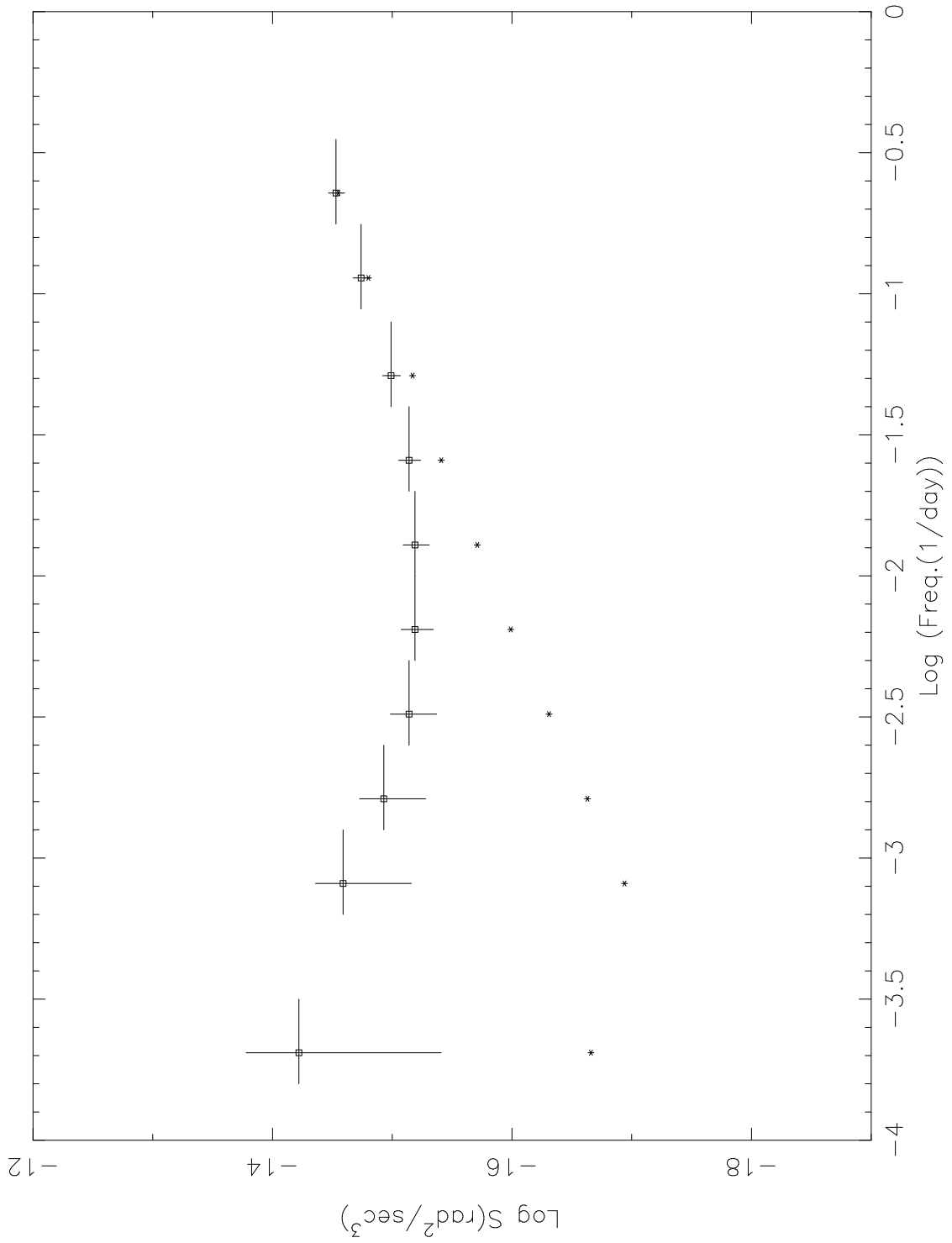


Fig. 3. | Power Spectrum of angular accelerations (or noise strengths, see the text)

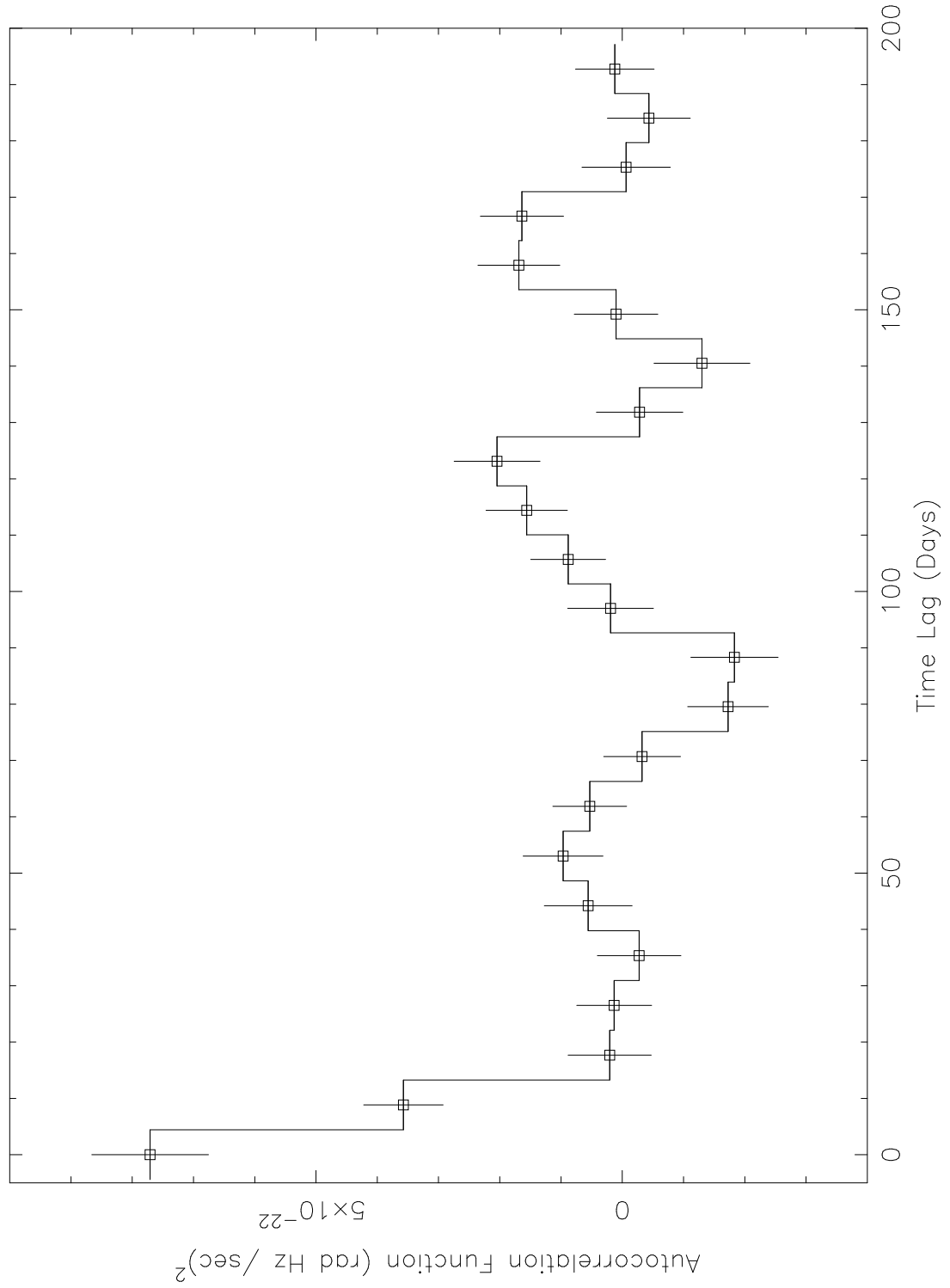
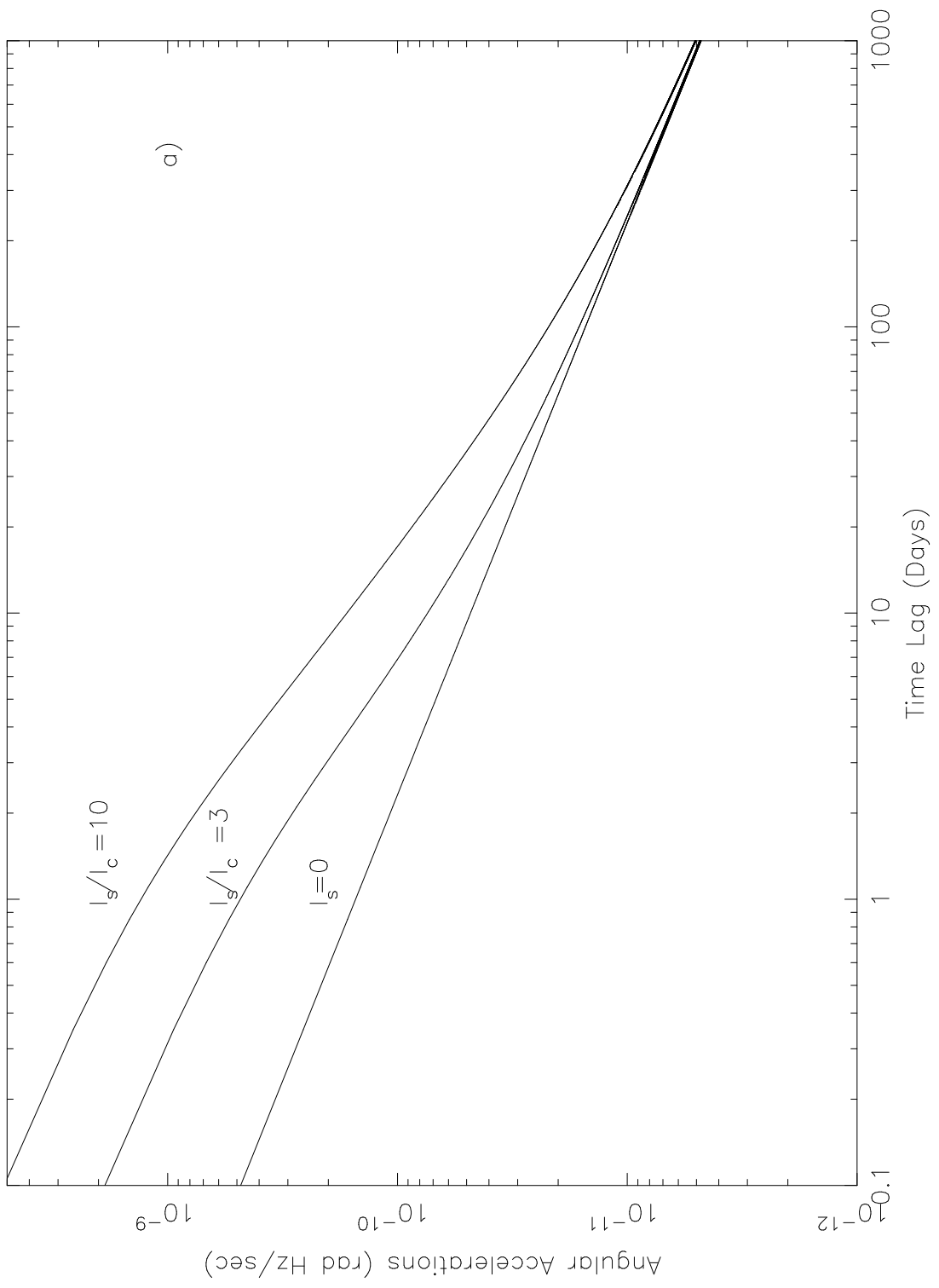
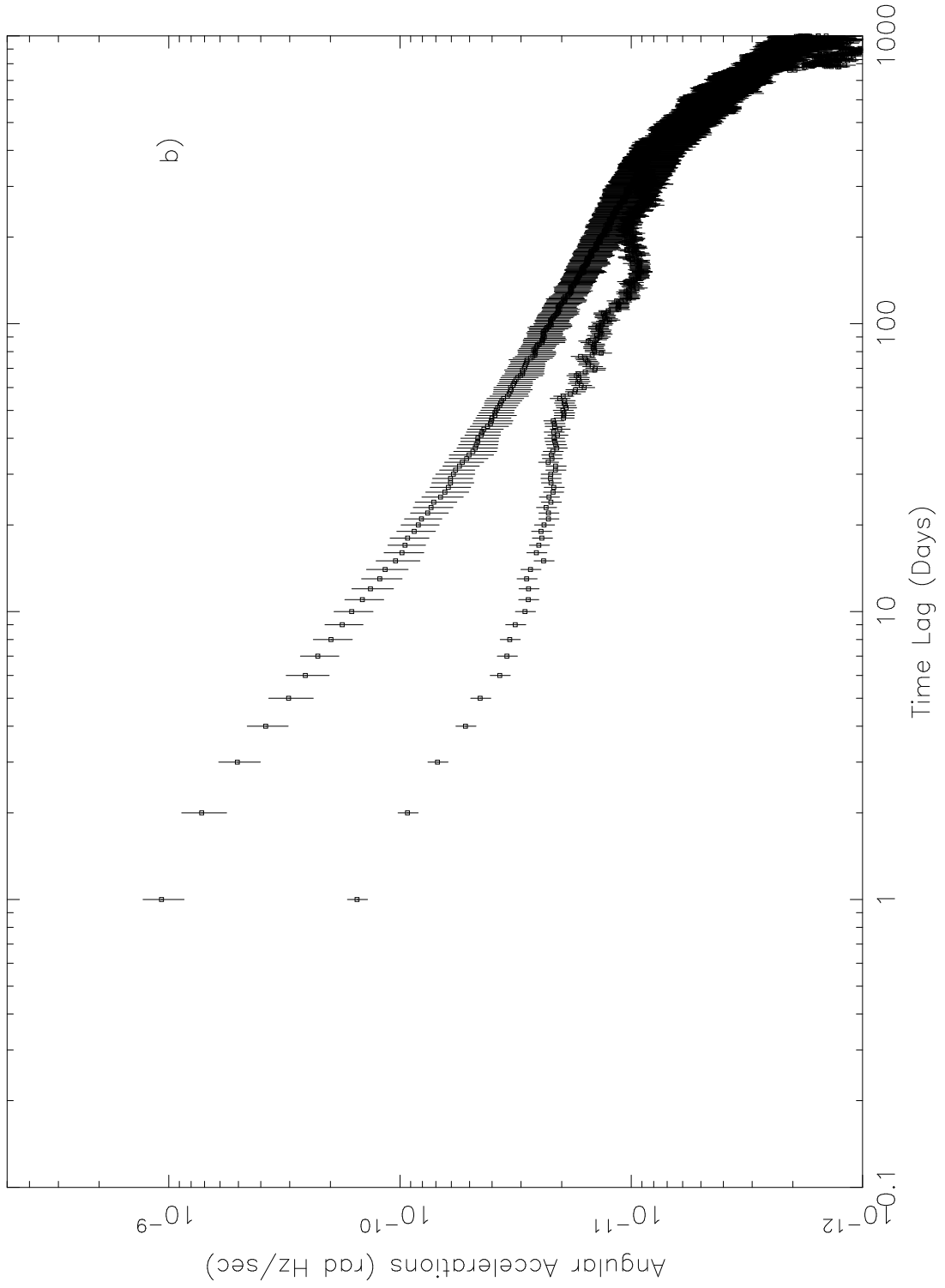


Fig. 4. | Autocorrelation function of angular accelerations time series.





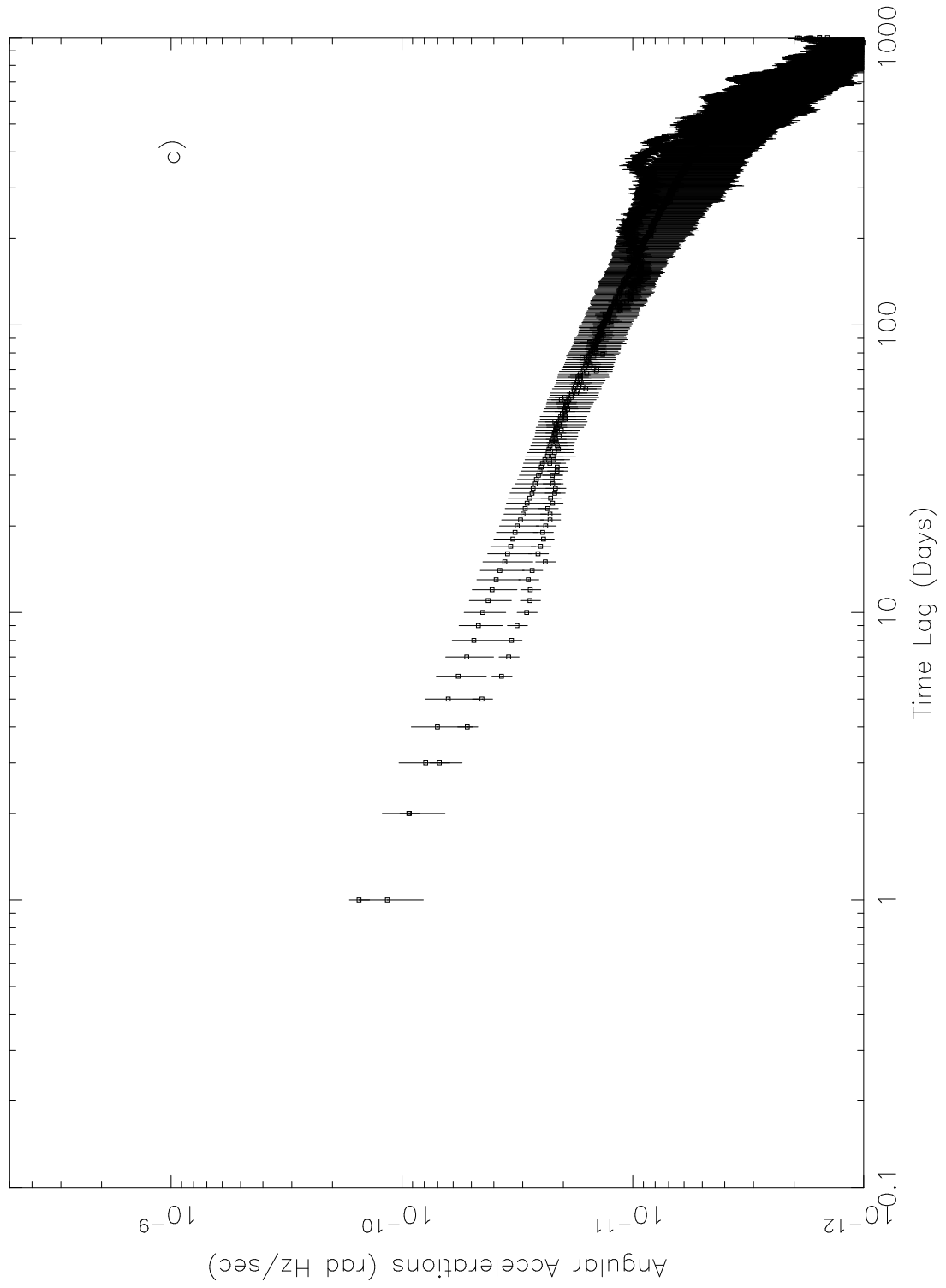


Fig. 5.

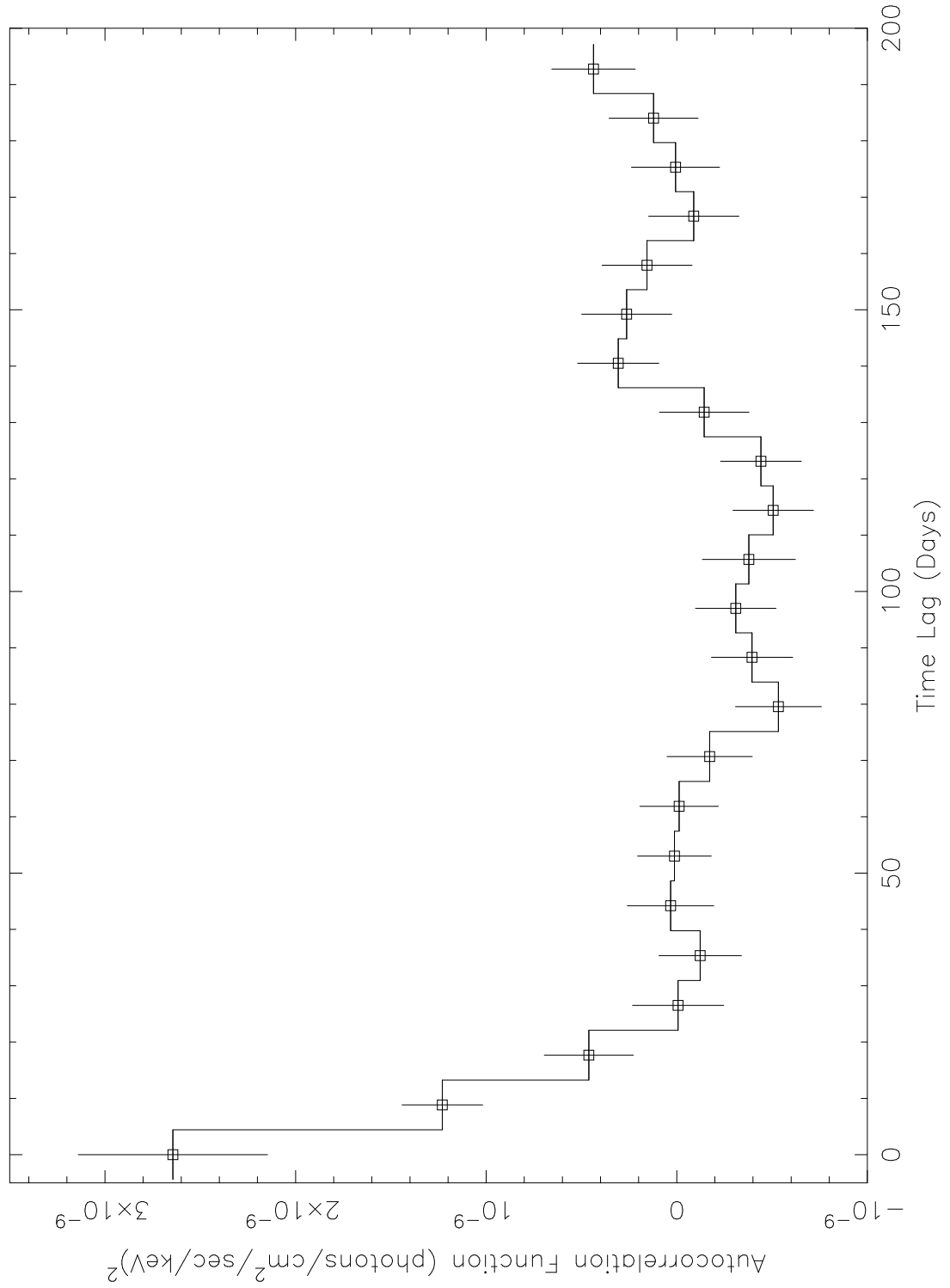
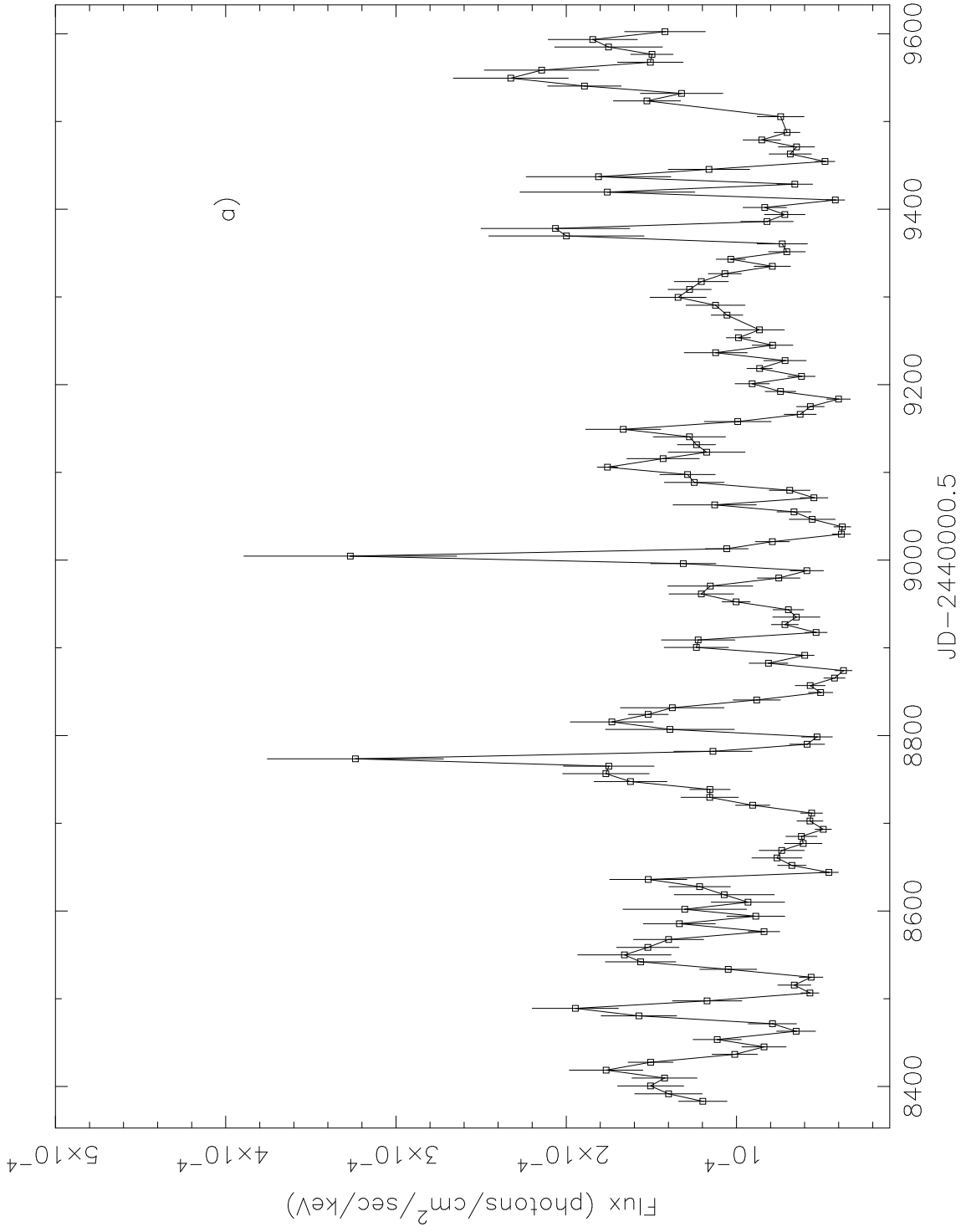
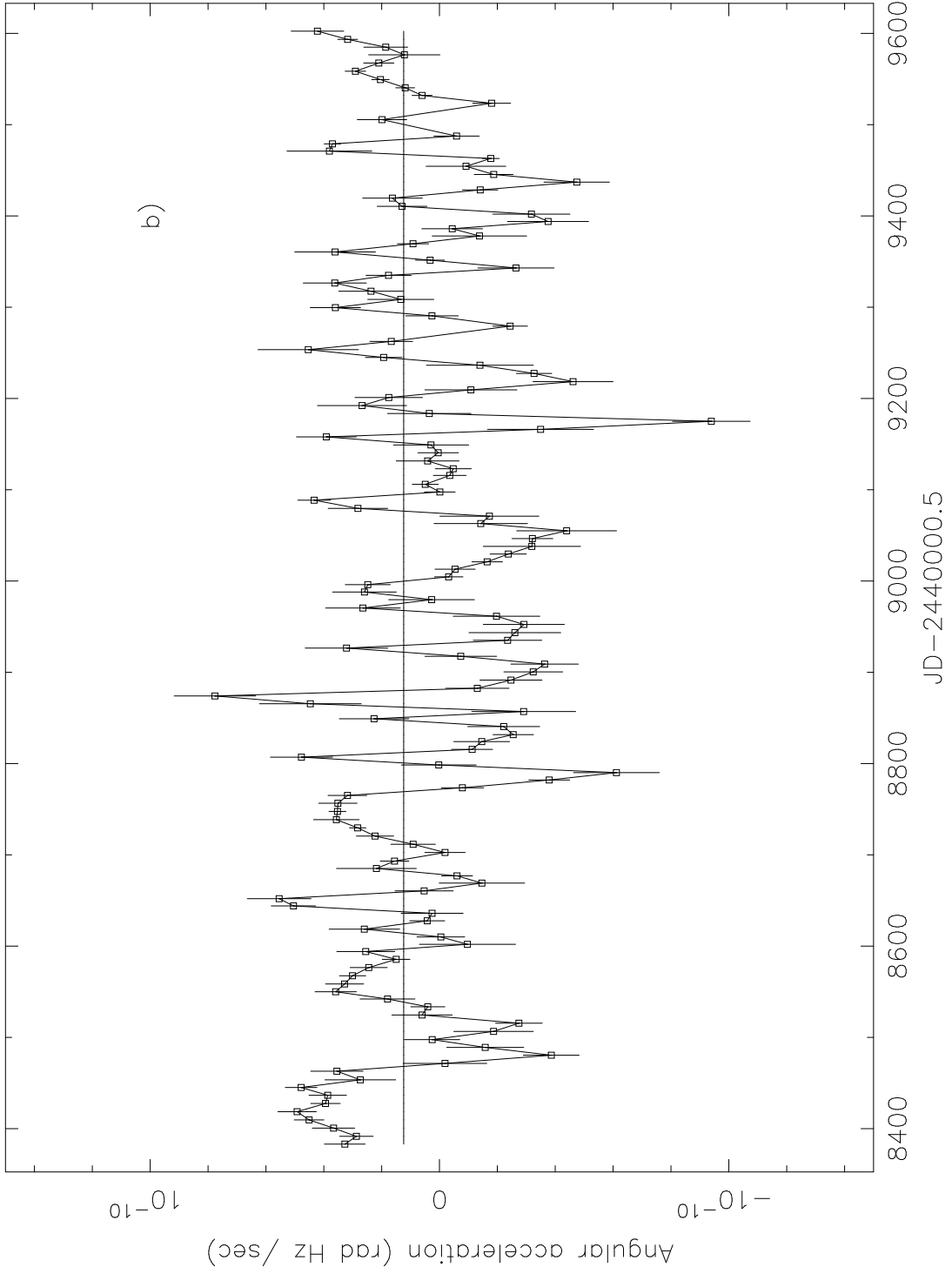


Fig. 6. | Autocorrelation function of pulse ux time series



CO= 1.2398E-11, W= 1582. , N= 139.0



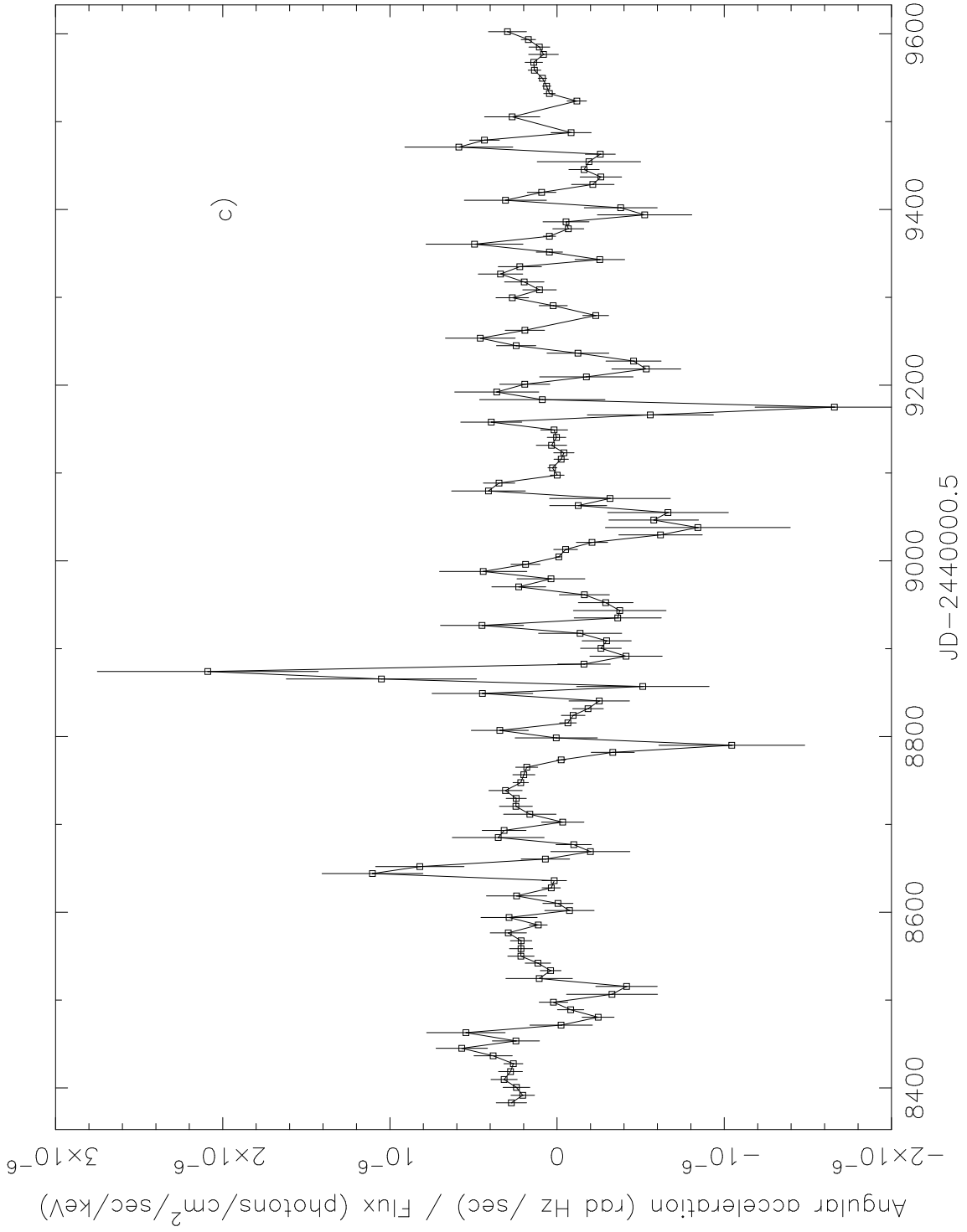
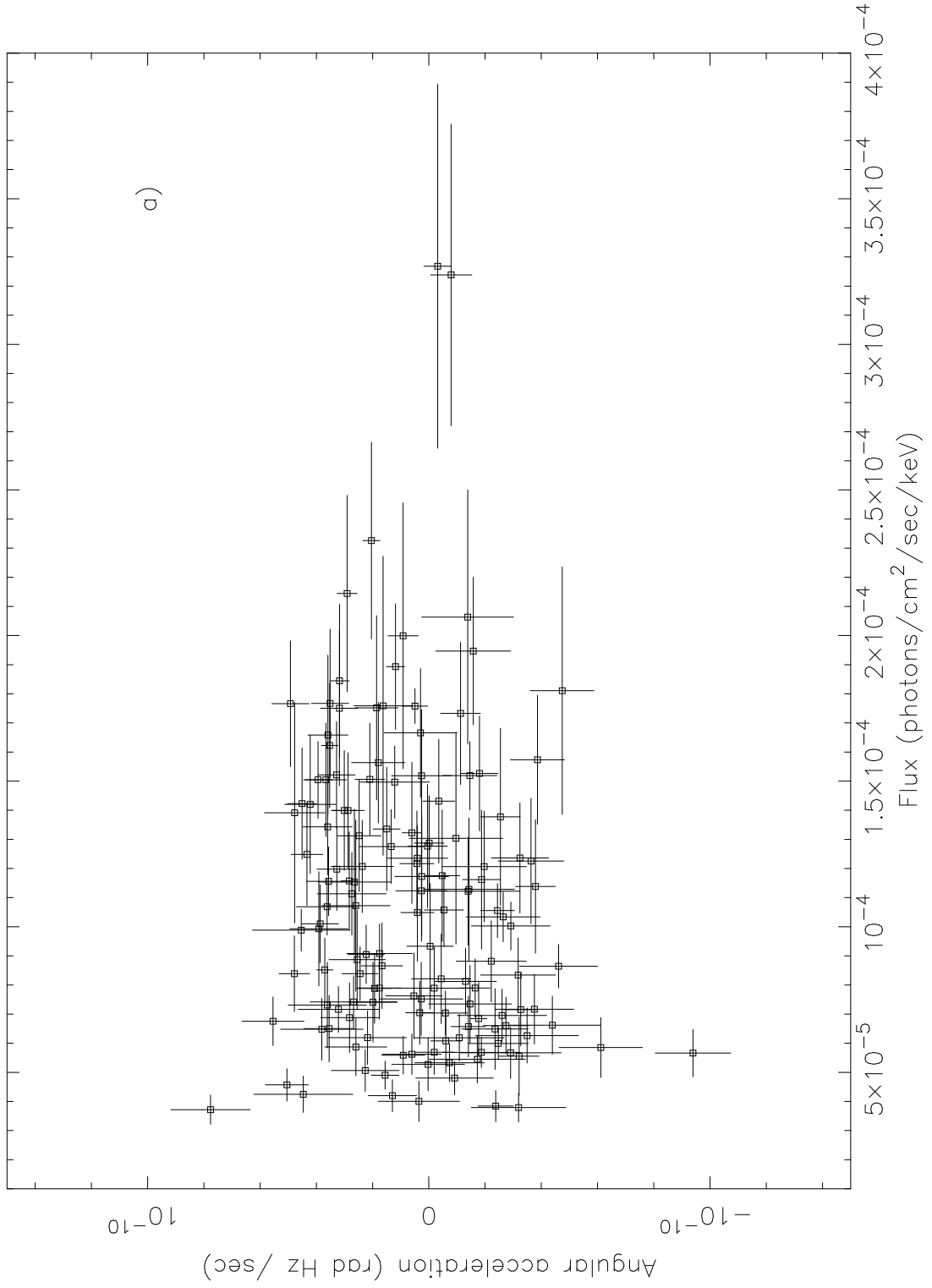
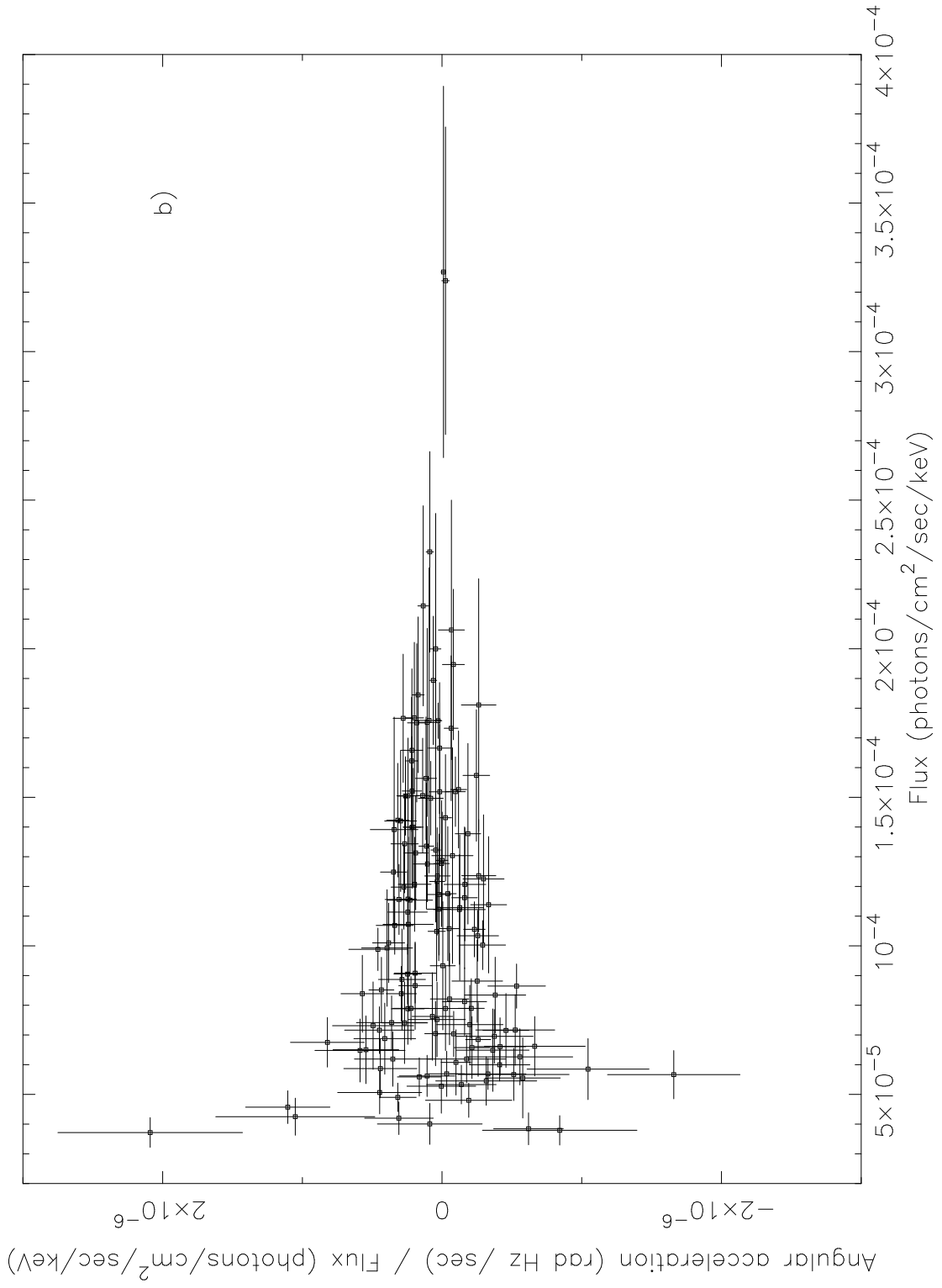


Fig. 7.





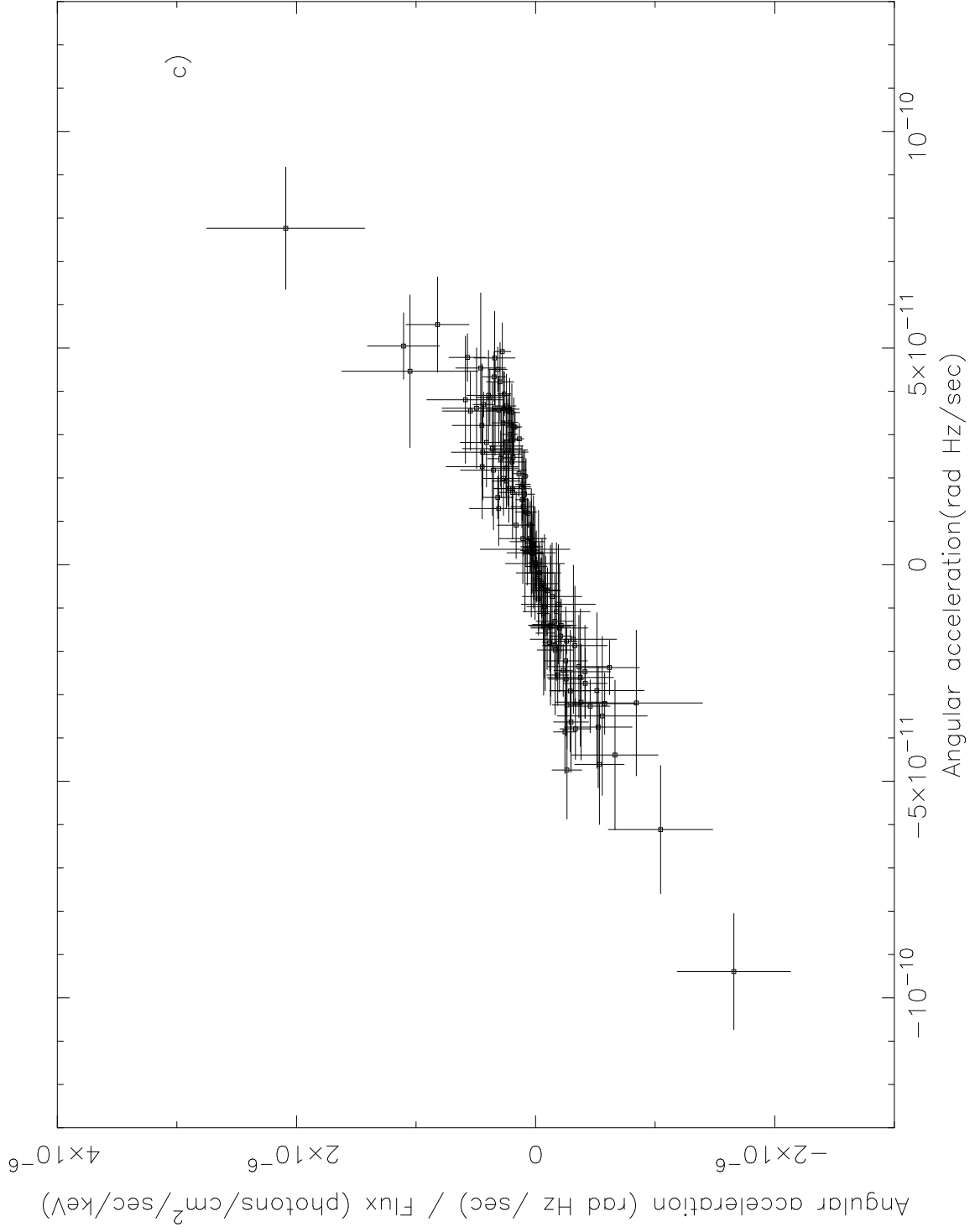


Fig. 8.